Ultramicroscopy 109 (2009) 781–787

Contents lists available at ScienceDirect

Ultramicroscopy

journal homepage: www.elsevier.com/locate/ultramic

Real space maps of atomic transitions

P. Schattschneider [a,c,*], J. Verbeeck [b], A.L. Hamon [c]

[a] Institut für Festkörperphysik, Technische Universität Wien, A-1040 WIEN, Austria
[b] EMAT, University of Antwerp, Groenenborgerlaan 171, B-2020 Antwerp, Belgium
[c] LMSSMAT, École Centrale Paris, Grande Voie des Vignes, F-92290 Chatenay-Malabry, France

ARTICLE INFO

Article history:
Received 17 September 2008
Received in revised form
8 January 2009
Accepted 13 January 2009

PACS:
79.20.Uv
68.37.Og
32.10.Dk
34.80.Nz

Keywords:
Electron energy loss spectrometry
Transmission electron microscopy
Circular dichroism
Coherence

ABSTRACT

Considering the rapid technical development of transmission electron microscopes, we investigate the possibility to map electronic transitions in real space on the atomic scale. To this purpose, we analyse the information carried by the scatterer's initial and final state wave functions and the role of the different atomic transition channels for the inelastic scattering cross section. It is shown that the change in the magnetic quantum number in the transition can be mapped. Two experimental set-ups are proposed, one blocking half the diffraction plane, the other one using a cylinder lens for imaging. Both methods break the conventional circular symmetry in the electron microscope making it possible to detect the handedness of electronic transitions as an asymmetry in the image intensity. This finding is of important for atomic resolution energy-loss magnetic chiral dichroism (EMCD), allowing to obtain the magnetic moments of single atoms.

1. Introduction

The new generation of transmission electron microscopes (TEMs) , equipped with aberration correctors, energy filters and monochromators provides exciting possibilities. It has been shown recently that the new microscopes bear indeed enormous potential for energy filtered images at atomic resolution (HR EFTEM) [1–3]. In that context, HR EFTEM attract particular interest. A notorious problem has been the combination of elastic and inelastic interaction, i.e. the propagation of the probe electron in the crystal potential before and after the inelastic event. Although theoretically solved [4–11], applications have remained elusive due to the huge computational effort. With a number of insights and proposals, theory has also made progress [12,13], providing advanced methods. It is therefore reasonable to investigate some of those details of electronic transitions that will be important for interpretation of results expected from last generation microscopes. Such considerations may also serve as a guide for future experiments and instrumental development.

In this paper we analyse the possibility to map electronic transitions on an atomic scale, focussing on the information that is contained in the initial and final state wave functions of the scatterer. We concentrate on the inelastic interaction part and calculate the wave function of the probe electron due to single atomic transition channels. In doing so, we derive the inelastic scattering kernel in real space. This treatment clarifies the role of the different channels in the scattering cross section, and makes contact to the density matrix approach [14]. Based on a recent proposal [15] it will be shown that the handedness of electronic transitions (which translates into the change in the magnetic quantum number $\Delta m = 0$ or ± 1) bear unique signatures that can be mapped in real space.

This situation occurs in energy-loss magnetic chiral dichroism (EMCD) experiments [16–18]. The particular attractivity of EMCD lies in the possibility to detect atom specific magnetic moments in combination with sum rules for the spin and orbital components [19,20] with nanometer resolution [21]. Whereas the standard EMCD geometry does not allow atomic resolution, it is shown that off-axis HR EFTEM conditions are more favourable. Imaging with a cylinder lens even allows the direct visualisation of the transferred angular momentum and its numerical evaluation on a per atom-basis.

Apart from the fundamental interest in the physics of the chiral and non-chiral transitions and its relationship to angular

* Corresponding author at: Institut für Festkörperphysik, Technische Universität Wien, A-1040 WIEN, Austria.
E-mail address: schattschneider@ifp.tuwien.ac.at (P. Schattschneider).

0304-3991/$ - see front matter © 2009 Elsevier B.V. All rights reserved.
doi:10.1016/j.ultramic.2009.01.016

momenta, the analysis will provide some ideas about unusual scattering geometries.

2. Basic considerations

After inelastic interaction, the probe electron is in a mixed state. That means that a density matrix [22,23] describes the system correctly. This concept has been proposed for fast electron scattering by Dudarev et al., [5] and further developed by Schattschneider et al. [14]. One may avoid the use of the density matrix in inelastic electron scattering by propagating the mutually incoherent wave functions of the probe to the detector, and adding the respective intensities. There is a caveat, however: in doing so, one loses information on the coherence between different positions on the detector; secondly, adding intensities instead of amplitudes one must be sure that there is no interference between the different terms.

It is convenient to separate the three-dimensional (3D) coordinates into z and $\mathbf{x}$ variables where the latter denote a two-dimensional (2D) position vector in a lateral plane. In the single inelastic scattering approximation, the density matrix of the inelastically scattered electron at the exit plane of the specimen ($z=d$) is

$$\rho_o(\mathbf{r}_o,\mathbf{r}'_o)=\int G_{d-z}(\mathbf{r}_o,\mathbf{x})G^*_{d-z'}(\mathbf{r}'_o,\mathbf{x}')T_{zz'}(\mathbf{x},\mathbf{x}') \times \rho_{zz'}(\mathbf{x},\mathbf{x}')\,dS_{\mathbf{x}}\,dS_{\mathbf{x}'}\,dz\,dz', \tag{1}$$

where $\mathbf{r}_o$ and $\mathbf{r}'_o$ are 2D variables for the positions in the exit planes, Green's function G_z propagates the electron after inelastic interaction in the crystal potential from $(\mathbf{x},z=0)$ to $(\mathbf{r},z)$ and T is the inelastic scattering kernel. $\rho_{zz'}(\mathbf{x},\mathbf{x}')$ is the density matrix of the incident electron at positions $\mathbf{x},z;\mathbf{x}',z'$ in the specimen. In single inelastic scattering approximation $\rho_{zz'}$ can be written as a product of wave functions: because there was no inelastic interaction before, the electron is still in a pure state

$$\rho_{zz'}(\mathbf{x},\mathbf{x}')=\psi_z(\mathbf{x})\psi^*_{z'}(\mathbf{x}') \tag{2}$$

with

$$\psi_z(\mathbf{x}):=\psi(\mathbf{x},z)=\int G_z(\mathbf{x},\mathbf{r}_i)\psi_i(\mathbf{r}_i)\,dS_{\mathbf{r}_i} \tag{3}$$

with $\mathbf{r}_i$ the lateral coordinate in the entrance plane of the specimen ($z=0$), and ψ_i the incident electron wave function.

Fig. 1 shows the position of the relevant planes in the specimen. The integral in Eq. (1) is over the whole 3D specimen.

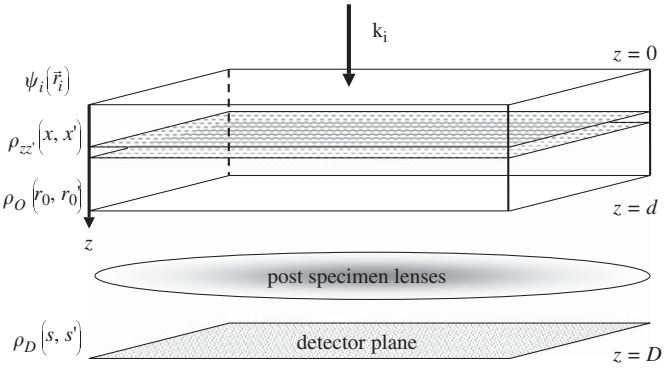

Fig. 1. Position of relevant planes in an inelastic scattering experiment: ψ_i with wave vector k_i at the entrance plane ($z=0$) with coordinates $\mathbf{r}_i$, $\rho_{zz'}$ at any depths z and z' within the specimen, and ρ_o at the exit plane ($z=d$). The detector is situated after the post specimen lens system in the plane ($z=D$) where lateral coordinates are $\mathbf{s}$ and $\mathbf{s}'$.

We should note that we have implicitly fixed the energy loss and omitted this variable for convenience.

Eq. (1) is valid in single inelastic scattering approximation, justified for core losses in specimens of usual thickness because the core excitation's mean-free path (MFP) is several hundred nm.

The density matrix $\rho_{zz'}$ can be calculated with any dynamical scattering code when the incident wave $\psi_i(\mathbf{r}_i)$ at the entrance surface $z=0$ is known. The density matrix ρ_o at the exit plane $z=d$, Eq. (1), is finally propagated to the detector via G_D describing the action of lenses and apertures. The intensity $I(\mathbf{s})$ is measured in the detector plane $z=D$. It is given by the diagonal elements of the density matrix (ρ_D)

$$I(\mathbf{s})=\rho_D(\mathbf{s},\mathbf{s})=\int G_D(\mathbf{s},\mathbf{r})G^*_D(\mathbf{s},\mathbf{r}')\rho_o(\mathbf{r},\mathbf{r}')\,dS_{\mathbf{r}}\,dS_{\mathbf{r}'}. \tag{4}$$

To resume, Eqs. (1)–(4) describe the inelastic scattering experiment completely.

3. Atomic transition channels in real space

In the following part, we adapt Eq. (4) to the case of single atom ionisation.

The propagator G_z depends on the energy of the probe electron. We can extract a rapidly varying phase factor and obtain

$$G_z(\mathbf{x},\mathbf{r})=\bar{G}_z(\mathbf{x},\mathbf{r})e^{ik_iz},$$

where $k_i=2\pi/\lambda_i$ is the incident electron's wave number. $\bar{G}_z$ is the propagator normally used in multislice calculations or in Bloch wave methods. When calculating elastic intensities, the phase factor cancels with its complex conjugate, so it is omitted in general. But in treating inelastic interactions we must keep it.

The propagator G_{d-z} applies to electrons after energy loss, that is, we can also extract a rapidly oscillating phase factor as previously for G_z:

$$G_{d-z}(\mathbf{x},\mathbf{r})=\bar{G}_{d-z}(\mathbf{x},\mathbf{r})e^{ik_o(d-z)}$$

with the outgoing electron's wave number k_o. We can now replace the propagators in Eq. (1) by the normally used ones for Bloch wave propagation

$$\rho_o(\mathbf{r}_o,\mathbf{r}'_o)=\int\int \bar{G}_{d-z}(\mathbf{r}_o,\mathbf{x})\bar{G}^*_{d-z}(\mathbf{r}'_o,\mathbf{x}')T_{zz'}(\mathbf{x},\mathbf{x}') \times \bar{\psi}^*_z(\mathbf{x})\bar{\psi}_{z'}(\mathbf{x}')\,dS_{\mathbf{x}}\,dS_{\mathbf{x}'}\,e^{iq_e(z-z')}\,dz\,dz', \tag{5}$$

where after extraction of the exponential factors the wave functions ψ of Eq. (3) are now replaced by

$$\bar{\psi}_z(\mathbf{x})=\int \bar{G}_z(\mathbf{x},\mathbf{r}_i)\psi_i(\mathbf{r}_i)\,dS_{\mathbf{r}_i} \tag{6}$$

and $q_E=k_o-k_i$ is the minimum wave vector transfer in the inelastic interaction. For energy losses of $<\sim$1 kV as encountered in EFTEM, the Bloch wave propagators $\bar{G}_z$ for the incident electron and $\bar{G}_{d-z}$ for the inelastically scattered electron can be assumed to be equal, which may simplify the calculations. (Note that this is not the case for G because of the different phase factors.) We have expressed the z dependence explicitly in preparation for the next step. The inelastic scattering kernel T can be written in configuration space as the convolution of the mixed dynamic form factor (MDFF) [4] S with the Coulomb coupling field [24] $R^{-1}=1/|\mathbf{R}|$ where $\mathbf{R}$ is the configuration space vector $\mathbf{R}=(\mathbf{x},z)$

$$T_{zz'}(\mathbf{x},\mathbf{x}')=S(\mathbf{R},\mathbf{R}')\star(R^{-1}R'^{-1}). \tag{7}$$

Assuming that we have a plane wave incident parallel to the optical axis, and a single atom in the object plane of a perfect lens, then $G_D(\mathbf{s},\mathbf{r}_o)=\delta^2(\mathbf{s},\mathbf{r}_o)$, and $G_{d-z}(\mathbf{r}_o,\mathbf{x})=\delta^2(\mathbf{r}_o,\mathbf{x})$, where δ^2 is the